Experimental Investigation on Joining of DP590–DP980 Automotive Steels by Resistance Spot Welding

S. U. Ghunage and B. B. Ahuja

1 Introduction

With the advent of newer and newer materials, the automotive industry has shifted its focus on the reduction of the vehicle weight and increment in the mileage without compromising the safety of passengers. For modern vehicular construction, a wide variety and grades of materials are needed to join together. Therefore, dissimilar metal welding is gaining momentum in the welding industry. For structural applications, it is required to join sheets of materials with different mechanical, metallurgical, and electrical properties. The difference in the properties of dissimilar metals results in challenges in obtaining the sound welds.

In recent years, Dual-Phase (DP) Steels have been practiced in the fabrication of vehicular components such as chassis, bumpers, vehicle frames, and wheel rims. Advanced High-Strength Steels (AHSSs) are a type of steel that combines high strength and ductility in one composition. These characteristics make them useful in automotive applications where higher values of strength and crash resistance are required while using thinner gauge parts. Higher fracture strain indicates good formability. The microstructure of DP steel consists of ferrite and martensite, which offers superior strength and excellent formability.

For the welding of dissimilar metals using the spot welding technique, the effect of welding time has been carried out by Bina et al. They have studied the weldability of austenitic stainless steel (AISI304) with ferritic stainless steel using Resistance Spot Welding. Optimum welding time for welding was obtained considering weld force and weld current constant [1]. Pouranvari et al. have presented a detailed review

S. U. Ghunage (✉) · B. B. Ahuja
Department of Manufacturing Engineering and Industrial Management, College of Engineering, Pune 411 005, India
e-mail: sug.mfg@coep.ac.in

B. B. Ahuja
e-mail: bba.mfg@coep.ac.in

N. Ramesh Babu et al. (eds.), *Advances in Additive Manufacturing and Metal Joining*, Lecture Notes in Mechanical Engineering,
https://doi.org/10.1007/978-981-19-7612-4_35

of spot welding of automotive steels. The authors have reviewed metallurgical characterizations of the welded joints [2]. Aydin investigated the mechanical and metallurgical characteristics of dissimilar metal joints of DP600 and DP1000 steels. He has observed that better mechanical and metallurgical properties were obtained at a welding current of 10 kA [3]. Valera used Resistance Spot Welding for welding sheets of micro-alloyed steels (TRIP) and found optimal electrical parameter values for obtaining sound weld strength of the speciemen [4]. Khan et al. have carried out a comparative study of welding of DP600 sheets using Resistance Spot Welding and Friction Stir Spot Welding [5]. Muhammad et al. have used the multi-objective Taguchi technique and response surface methodology to evaluate performance and to improve quality in Resistance Spot Welding [6]. Hwang et al. have investigated the weldability of DP780 steels. Experiments were carried out using AC-type and DC-type resistance spot machines [7]. Further researchers explored the combinations of different materials for dissimilar metal joining using Resistance Spot Welding and further investigated the affectability of variation in input process parameters on weld strength and failure modes effectively [8–10].

As per the literature review, researchers have welded DP steels with similar DP steels and different grades of DP steels. Major work has been reported for laser welding of DP780 and DP980 high-strength steel joints, Friction Stir Welding of DP590 steel, and Resistance Spot Welding of DP590 steels. However, no significant work has been reported using Resistance Spot Welding for joining of DP590 and DP980 steels. Therefore, the objective of the research work was to examine the weld characteristics of DP590 and DP980 steels and also to evaluate relation of input process parameters for greater weld strength of these joints.

2 Materials and Experimental Procedure

In this work, dissimilar metals (DP980 and DP590) have been joined using Resistance Spot Welding. Sheets of Dual-Phase Steels DP980 and DP590 having thickness 1.2 mm have been used for the experimental work. As per ASTM E8 standards, the sample size of the weld specimen was chosen as 80 × 20 mm and the overlap was kept equal to the width of the specimen, i.e., 20 mm.

The specimen required for the welding operation was cut in the direction of the rolling of the plates. Before welding operation, to eliminate dirt, surface scale, oxide layer, the specimen was carefully cleaned using ethanol. As the joint is of overlap type, for the weld combination, the DP980 plate is kept on the upper side and the DP590 plate is kept on the lower side. The welding process was carried out by using an RSW machine (KEJE make) having 25 kVA capacity as shown in Fig. 1. The machine was equipped with a controller (AMADA make) which controls the welding, squeezing, and holding cycles during the welding process. To ensure correct alignment of the overlapping plates and its stability during the welding process, a welding fixture has been used. The electrodes used for the RSW process are Cu–Cr alloy electrodes. These electrodes were water-cooled and had a tip diameter of 7 mm.

Fig. 1 Spot welding machine (KEJE make) used for experimentation

The chemical composition of DP590 and DP980 steels is indicated in Table 1. The mechanical properties of DP590 and DP980 steels are indicated in Table 2. From the screening experiments, three factors and three levels of welding current, electrode force, welding time are chosen for the study as indicated in Table 3. The experiments are conducted using Taguchi's L_{27} orthogonal array.

Table 1 Chemical composition of DP580 and DP980 steels

Steel	C	Mn	Si	Cu + Cr + Ni	Cr	Fe
DP590	0.12	1.6	0.4	1.3	–	Balance
DP980	0.177	1.38	1.42	–	0.44	Balance

Table 2 Mechanical properties of DP580 and DP980 steels

Steel	Yield strength (MPa)	Tensile strength (MPa)	% Elongation
DP590	360	610	23
DP980	650	1010	13.5

Table 3 Process parameters with their levels

Parameter	Levels		
Electrode force (kN)	2	3	4
Weld time (cycles)	8	12	16
Welding current (kA)	6	7	8

3 Design of Experiments

To determine the governing parameters inherent with any process, the Design of Experiments (DOE) methodology is effectively used by researchers. It helps in finding the optimal settings for these process parameters. With optimized parameters, the process yields higher performance and ensures better capability [11].

In this work, for the joining of DP590 and DP980 steels, the process parameters electrode force, weld cycles, and welding current are considered. Its effect on mechanical properties like tensile shear strength and indentation depth of weld metal has been evaluated. The three-level Full Factorial (3^n) method is adopted to design the experimental work. The total number of the experiments (27) is carried out. For the different levels, different values of the input parameters used in the experiment are tabulated in Table 3.

As per the design matrix, the 27 sets of trials are carried out. The samples for the tensile test are prepared as per the ASTM E8 standard. The data are used then to develop a mathematical model using the Design of Experiments (DOE) method [12]. The result of failure load and indentation of the electrode are shown in Table 4.

From Table 4, it is observed that for the higher values of current and weld cycles, the values of failure load were on higher side. The highest value of failure load was observed at 8 kA of current, 16 cycles of weld time, and 2 kN electrode force. A similar higher value of failure load was also observed at 8 kA of current, 16 cycles of weld time, and 4 kN electrode force, however, occurrence of splashing and arcing between the adjoin plates of the workpiece Fig. 2.

To investigate joint strength of the welded specimen, the tensile shear test was carried out. It was observed that the occurrence of fracture in the region of the base metal of DP590 than the heat-affected zone (HAZ) region. Failure modes for these welded samples were of mixed type, i.e., few samples where current and weld cycles were at the lowest level, and the interfacial mode of failure was observed as indicated in Fig. 3a and b respectively. On the contrary, for the higher value of weld current and weld cycles, the weld nugget was on the higher side and the failure mode was pullout type as indicated in Fig. 4a and b respectively.

The weld strength/failure load and indentation depth have been considered as response parameters. The output responses were analyzed using Minitab V17 and the main effect plots are shown in Figs. 5 and 6, respectively.

From the Design of Experiments, among the chosen factors for the study, it was inferred that welding current is the most dominating factor controlling the failure load or weld strength followed by weld cycles. The study also reveals that the weld force is the least influencing factor.

The depth of electrode penetration on the sheets governs the mechanical characteristics of the welded specimen. The contributing factors of the depth of penetration by electrodes on the sheets were the electrode pressure and temperature of the electrode–sheet interface. As the heat input increases, the temperature of the electrode–sheet interface also increases, causing higher degree of plastic deformation. In case of severe electrode indentation, the occurrence of expulsion was observed. It was

Table 4 Failure load and indentation of electrode

Weld schedule	Force (kN)	Weld time (cycles)	Welding current (kA)	Indentation (mm)	Failure load (N)
1	2	8	6	0.175	8440
2	2	8	7	0.238	9300
3	2	8	8	0.266	9900
4	2	12	6	0.203	9640
5	2	12	7	0.371	10,000
6	2	12	8	0.298	10,713
7	2	16	6	0.204	9760
8	2	16	7	0.349	10,438
9	2	16	8	0.332	11,050
10	3	8	6	0.192	8400
11	3	8	7	0.161	9100
12	3	8	8	0.226	9690
13	3	12	6	0.242	9280
14	3	12	7	0.266	9950
15	3	12	8	0.241	10,413
16	3	16	6	0.239	9590
17	3	16	7	0.297	9700
18	3	16	8	0.350	10,838
19	4	8	6	0.114	8120
20	4	8	7	0.157	8640
21	4	8	8	0.212	9690
22	4	12	6	0.201	9100
23	4	12	7	0.304	9920
24	4	12	8	0.287	9910
25	4	16	6	0.227	9540
26	4	16	7	0.307	10,288
27	4	16	8	0.377	11,050

ascertained that the welding current affects the electrode indentation comparatively more than that of the welding time.

The amount of indentation depth is deciding factor for mechanical properties and nugget size of the welded specimen. Therefore, the depth of electrode penetration is considered as the second response parameter. The output response is analyzed using Minitab V17 and the main effect plot is shown in Fig. 6.

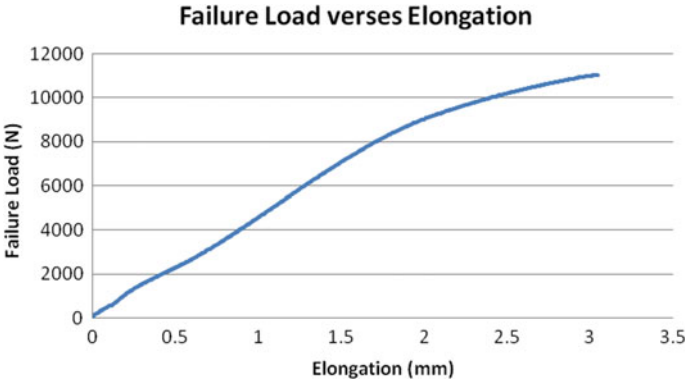

Fig. 2 Failure load versus elongation curve for DP590–DP980 welded specimen

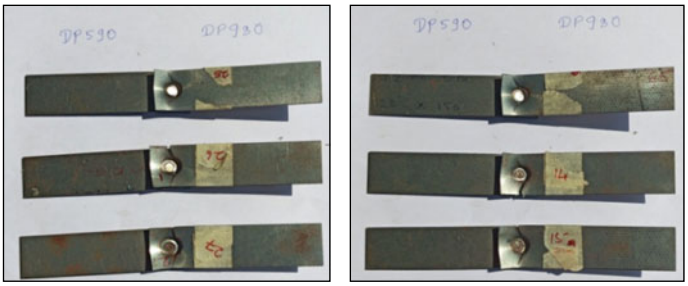

DP590-DP980 (a) DP590-DP980 (b)

Fig. 3 Interfacial failure mode of the welded specimen (**a** and **b**)

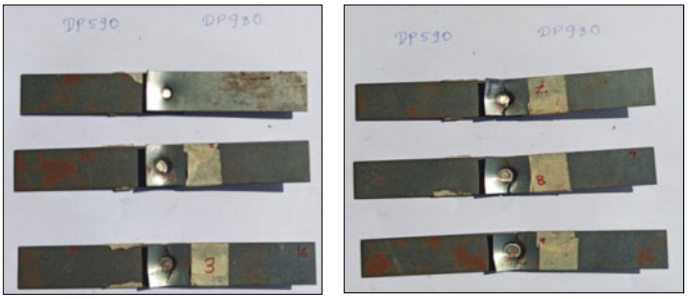

DP590-DP980 (a) DP590-DP980 (b)

Fig. 4 Pullout failure mode of the welded specimen (**a** and **b**)

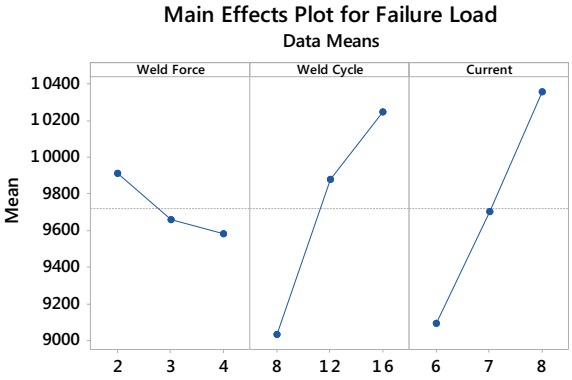

Fig. 5 Mean of S/N ratios for failure load

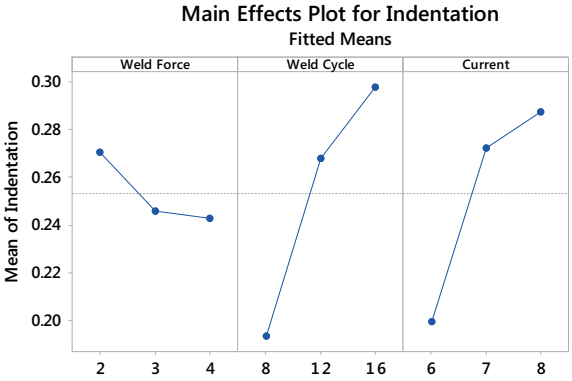

Fig. 6 Mean of S/N ratios for indentation

4 Analysis of Variance

For the Resistance Spot Welding of dissimilar materials, the quality characteristics of tensile shear strength of the welded specimens indicate the larger-the-better type. The result of ANOVA for the welding responses is presented in Table 5. The larger the *F*-value indicates major changes in the rank of the welding parameters. From Table 5, it can be concluded that welding current and weld cycles were the most influencing parameters affecting the responses, whereas the electrode force was comparatively less influencing.

For the higher values of welding current (8 and 9 kA) and weld cycles (12 and 16 cycles), the tensile shear strength of the weld specimen was higher. However, the values of tensile shear strength decrease as the electrode force increases from 2 to 4 kN. For Resistance Spot Welding (RSW) process, from the analysis, it was revealed that the governing parameter that influences the tensile shear strength was welding current with 46.07% contribution. The second important parameter that influences the tensile shear strength was weld cycles with a 44.99% contribution. The weld force was with marginal contribution (3.46%) in deciding the tensile strength.

Table 5 ANOVA for the tensile shear load of DP590–DP980

Source	DF	Seq SS	Contribution (%)	*F*-value	*P*-value
Weld force	2	540,404	3.46	6.44	0.022
Weld cycles	2	7,035,762	44.99	83.88	0.000
Current	2	7,203,531	46.07	85.88	0.000
Error	8	335,515	2.15		

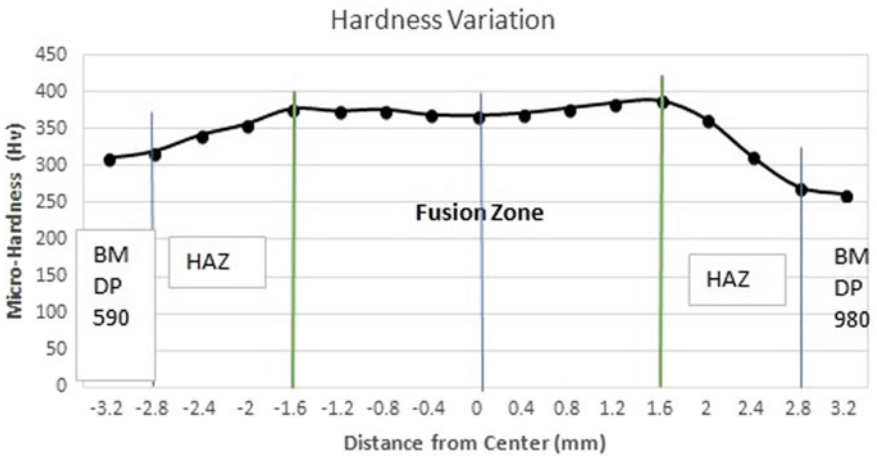

Fig. 7 Microhardness of dissimilar weld nugget (DP590–DP980)

The measurement of microhardness was carried out using Future-Tech FM700 Hardness Testing Machine. Figure 7 represents the microhardness measurement of the joint obtained by Resistance Spot Welding for the weld specimen which was obtained for weld schedule 9 (Force 2 kN, weld cycles 16, and current 8 kA). The load applied was 100 gm and dual time was 10 s.

The cross-section of dissimilar weld joints (DP590–DP980) revealed three main microstructural zones like base metal (BM), heat-affected zone (HAZ), and fusion zone (FZ). A fusion zone or weld nugget is a zone that undergoes melting during the welding process. In addition to this, the DP980 side of the joint was with a transition zone which lies between the heat-affected zone and the base metal. It has been also observed that softening of the zone has occurred to higher levels. A similar soft transition zone was not observed on the DP590 side. Higher hardness values were observed in the fusion zone of the nugget, followed by heat-affected zones, and lesser values were found in the base metal as indicated in Fig. 7.

5 Conclusions

In the present study, the mechanical characteristics of dissimilar DP590–DP980 steel joints were experimentally investigated using Resistance Spot Welding. To investigate the optimal values of process parameters, Taguchi DOE has been effectively employed. From the analysis, it is inferred that by increasing the welding current from 6 to 8 kA, the tensile shear strength of the welded joints increased linearly. The peak values of tensile shear strength are observed at welding current 8 kA and weld cycles 16. The failure locations of the joints were at heat-affected zones (HAZ). The joints failed at DP980 side when the welding currents are increased to an 8 kA value, while the failure was on the DP590 side for a higher current range. The contribution of welding current, weld cycles, and electrode force toward tensile strength is 46.07%, 44.99%, and 3.46%, respectively. From the ANOVA analysis, it can be observed that the *P*-value for experimented variables, welding current, and weld cycles are not higher than 0.05. Therefore, these terms are significant on the sensitivity of the process. Using the Taguchi method, it is inferred as optimal values for welding of DP980 and DP580 sheets are welding current 8 kA, weld cycles as 16, and electrode force as 2 kN.

From the experimental work carried out for DP590–DP980 steels, the conclusions can be summarized as below.

1. For the welded joints of DP590–DP980 steels, the weld cross-section shows three distinct zones as base metals, heat-affected zones of both the steels, and fusion zone. On the DP980 side, a transition zone was also visible in between BM and HAZ.
2. Mechanical and metallographic characterization of welded joints was carried out using tensile testing and hardness mapping.
3. To achieve the mechanically sound welds, the welding current was the most influencing parameter followed by weld cycles.
4. As the values of welding current and weld cycles increase, the tensile properties of the welded joints have increased significantly.
5. Pullout failure mode was observed for most of the tested samples and fracture has occurred at base metal indicating good weld strength.
6. The highest values of microhardness are observed in the fusion zone of the welded specimen. However, for the DP980 side, the lowest values were obtained in the transition zone.

Acknowledgements The authors express their sincere thanks to *Magna Automotive India Private Limited*, *Pune*, for providing the Dual-Phase Steel sheets and *Auto Cluster Development and Research Institute Centre (ACDRI)*, *Pune*, for providing the testing facilities.

References

1. Bina, M.H., Jamali, M., Shamanian, M., Sabet, H.: Effect of welding time in the resistance spot welded dissimilar stainless steels. Trans. Indian Inst. Met. **68**, 247–255 (2015)
2. Pouranvari, M., Marashi, S.P.H.: Critical review of automotive steels spot welding: process, structure and properties. Sci. Technol. Weld. Join. **18**, 361–403 (2013)
3. Aydin, H.: The mechanical properties of dissimilar resistance spot-welded DP600-DP1000 steel joints for automotive applications. Proc. Inst. Mech. Eng. Part D J. Automob. Eng. **229**, 599–610 (2015)
4. Valera, J., Miguel, V., Martínez, A., Naranjo, J., Cañas, M.: Optimization of electrical parameters in resistance spot welding of dissimilar joints of micro-alloyed steels TRIP sheets. Proc. Manuf. **13**, 291–298 (2017)
5. Khan, M.I., Kuntz, M.L., Su, P., Gerlich, A., North, T., Zhou, Y.: Resistance and friction stir spot welding of DP600: a comparative study. Sci. Technol. Weld. Join. **12**, 175–182 (2007)
6. Muhammad, N., Manurung, Y.H., Hafidzi, M., Abas, S.K., Tham, G., Rahim, M.R.A.: A quality improvement approach for resistance spot welding using multi-objective Taguchi method and response surface methodology. Int. J. Adv. Sci. Eng. Inf. Technol. **2**, 215 (2012)
7. Hwang, I., Kim, D., Kang, M., Kwak, J.H., Kim, Y.M.: Resistance spot weldability of lightweight steel with a high Al content. Met. Mater. Int. **23**, 341–349 (2017)
8. Vignesh, K., Perumal, A.E., Velmurugan, P.: Resistance spot welding of AISI-316L SS and 2205 DSS for predicting parametric influences on weld strength—experimental and FEM approach. Arch. Civ. Mech. Eng. **19**, 1029–1042 (2019)
9. Zhang, H., Qiu, X., Xing, F., Bai, J., Chen, J.: Failure analysis of dissimilar thickness resistance spot welded joints in dual-phase steels during tensile shear test. Mater. Des. **55**, 366–372 (2014)
10. Karuthapandi, K, Ramu, M., Thyla, P.R., Anantharuban, K.: Weld bead characterization of flat wire electrode in GMAW process part II: a numerical study. **35**(5), 1–8 (2021)
11. Thakur, A.G., Nandedkar, V.M.: Application of Taguchi method to determine resistance spot welding conditions of austenitic stainless steel AISI 304. J. Sci. Ind. Res. (India) **69**, 680–683 (2010)
12. ASTM E8: ASTM E8/E8M standard test methods for tension testing of metallic materials 1. Annu. B. ASTM Stand. **4**, 1–27 (2010)